УДК 539.172.12

«THERMAL» MULTIFRAGMENTATION IN p + Au COLLISIONS AT RELATIVISTIC ENERGIES

S.P.Avdeyev, V.A.Karnaukhov, W.D.Kuznetsov, L.A.Petrov, V.K.Rodionov, A.S.Zubkevich, H.Oeschler[1], O.V.Bochkarev[2], L.V.Chulkov[2], E.A.Kuzmin[2], A.Budzanovski[3], W.Karcz[3], M.Janicki[3], E.Norbeck[4], A.S.Botvina[5]

Multiple emission of intermediate-mass fragments has been studied for the collisions p + Au at 2.16, 3.6, and 8.1 GeV with the FASA set-up. The mean IMF multiplicities are equal to 1.7, 1.9, and 2.1 (± 0.2) respectively. The multiplicity, charge distributions and kinetic energy spectra of IMF are described in the framework of the empirically modified intranuclear cascade model followed by the statistical multifragmentation model. The results support a scenario of true thermal multifragmentation of a hot and expanded target spectator.

The investigation has been performed at the Laboratory of Nuclear Problems, JINR.

«Тепловая» мультифрагментация в соударениях p + Au при релятивистских энергиях

С.П.Авдеев и др.

Множественная эмиссия фрагментов промежуточной массы была исследована с помощью установки ФАЗА для соударений p + Au при 2,16; 3,6 и 8,1 ГэВ. Найдено, что средние множественности ФПМ соответственно равны 1,7; 1,9 и 2,1 (± 0.2). Распределения по множественности и заряду, а также спектры кинетических энергий ФПМ описываются в рамках эмпирически модифицированной модели внутриядерного каскада, сопровождаемой статистической моделью мультифрагментации. Результаты согласуются со сценарием тепловой мультифрагментации горячего спектатора мишени с пониженной плотностью.

Работа выполнена в Лаборатории ядерных проблем ОИЯИ.

Introduction

The investigation of the decay of very hot nuclei has become a topic of great interest. It is largely concentrated on the process of multiple emission of intermediate mass fragments (IMF, $3 \leq Z \leq 20$) [1–3]. Now it is established as the main decay mode of highly

[1]Institut für Kernphysik, TH Darmstadt, 64289, Germany.
[2]Kurchatov Institute, 123182 Moscow, Russia.
[3]H.Neiwodniczanski Inst. of Nuclear Physics, 31-342, Cracow, Poland.
[4]University of Iowa, Iowa City, IA 52242, USA.
[5]Institute for Nuclear Research, 117312, Moscow, Russia.

excited nuclei, and this process is likely to occur when a nucleus has expanded and lower density is reached. It is under debate whether this process is related to a liquid-gas phase transition in nuclear matter. The common way to produce very hot nuclei is to use reactions induced by heavy ions at energies 30–100 MeV/nucleon. But in this case heating is accompanied by compression, strong rotation and shape distortion, which cause the so-called dynamic effects in the nuclear decay. It seems difficult to disentangle all these effects to get information on the thermodynamic properties of a hot nuclear system. The picture becomes clearer when light relativistic projectiles are used [4–10]. One should expect that dynamic effects are negligible in that case. A further advantage is that all the IMF's are emitted by the only source — the target spectator, and decay of this hot nucleus proceeds in an apparently statistical manner («thermal multifragmentation»).

The time scale of the IMF emission is a key characteristic for understanding the multifragmentation phenomenon: is it a «slow» sequential process of independent emission of IMF's or is it a new decay mode with «simultaneous» ejection of the fragments governed by the total accessible phase-space? «Simultaneous» means that all fragments are liberated at freeze-out during a time, which is smaller than a characteristic Coulomb time τ_c. For that case emission of IMF's is not independent, they interact via long-range Coulomb forces during acceleration in the electrical field after freeze-out. According to [11], $\tau_c \approx 10^{-21}$ s. Measurement of the emission time for IMF's (τ_{em} is a mean time delay between two consecutive fragment emissions) is a direct way to answer the question as to the nature of the multifragmentation phenomenon. In our papers [12,13] it was found by measuring the relative angle IMF-IMF correlations that for ^{4}He + Au collisions at 14.6 GeV the emission time is less than $3 \cdot 10^{-22}$ s. The trivial mechanism of multiple IMF emission (sequential and independent evaporation) should be definitely excluded. So, the thermal multifragmentation is a new (multibody) decay mode of excited nuclei.

In this paper we present the experimental study of the multifragment emission induced by relativistic protons (up to 8.1 GeV) in gold. The preliminary data were presented in [14].

Experimental Set-Up

The experiments were performed with a proton beam of the JINR synchrophasotron in Dubna at energies of 2.16, 3.6, and 8.1 GeV using the modified 4π-set-up FASA [15]. The main parts of the device are: (i) five ΔE (ion.ch.)$\times$ E(Si)-telescopes, which serve as a trigger for the readout of the system allowing measurement of the charge and energy distributions of IMF's at different angles. They are located at $\theta = 24°$, 68°, 87°, 112°, and 156° to the beam direction and together cover the solid angle 0.03 sr; (ii) a fragment multiplicity detector (FMD) consisting of 64 CsI (Tl) counters (with thickness ranging from 20 to 27 mg·cm^{-2}), which cover 89% of 4π. The FMD gives the number of IMF's in the event and their space distribution. The plexiglass light guides [16] were replaced by hollow metal tubes with a diffuse reflector. This results in reducing the background in FMD (down to less than 2%) caused by the beam halo. It was continuously controlled by means of a

double-gate mode in PM-pulses processing [16]. The scintillator faces were covered by aluminized mylar (0.2 mg·cm^{-2}) to exclude completely the light cross-talk.

A self-supporting Au target 1.5 mg/cm^2 thick was located in the centre of the FASA vacuum chamber. The average beam intensity was $7 \cdot 10^8$ p/spill (spill length 300 ms, spill period 10 s). The blank-target background for telescopes in the angular range 65°–115° is around 5% for $Z_f = 2$ decreasing with Z_f to ≤ 1% for $Z_f \geq 6$.

In this work we revised the calculations of the efficiency of IMF registration by the scintillator counters. The modern data on the response function of CsI(Tl) to heavy ions [17] were used and self-absorption of light in polycrystalline CsI(Tl) [16] was taken into account. The pulse-height thresholds were set (actually off-line) in each counter individually depending on the scintillator thickness to get good separation of IMF from lighter fragments ($Z = 1,2$). The calculated efficiency of FMD for IMF detection is $\varepsilon = 59\%$ (instead of 46% used before), while the admixture of lighter particles to the counting rate is less than 5% with respect ot IMF's.

Fragment Multiplicity

The measured IMF-multiplicity distributions associated with a trigger fragment of charge $6 \leq Z \leq 20$ are shown in Fig.1a. The data were corrected for the admixture of lighter fragments and background in FMD. It was done using the random generator procedure. The mean associated multiplicities $\langle M_A \rangle$ for the beam energies 2.16, 3.6, and 8.1 GeV are equal to 0.73, 0.96, and 1.11 respectively. Note that the number of IMF detected is $1 + M_A$ (triggering fragment is added).

The measured distribution for the associated multiplicity $W(M_A)$ differs from the true (or primary) multiplicity distribution $W(M)$ because of distortion by triggering and because the FMD efficiency is less than 100%. These distributions are related via the response matrix of the FASA set-up $Q(M_A, M)$:

$$W(M_A) = \sum_{M = M_A + 1} Q(M_A, M)\, W(M). \tag{1}$$

The response matrix includes the triggering probability, which is proportional to M, and the probability of detecting (in FMD) M_A fragments from remaining $M - 1$. The latter probability is described by the binomial distribution. So, we have:

$$Q(M_A, M) = \frac{M!}{M_A!(M - 1 - M_A)!}\, \varepsilon^{M_A} (1 - \varepsilon)^{M - 1 - M_A}. \tag{2}$$

Using (1) and (2) one can find the following relation between $\langle M_A \rangle$ and the moments of the primary multiplicity distribution:

$$\frac{\langle M_A \rangle}{\varepsilon} = \frac{\langle M^2 \rangle}{\langle M \rangle} - 1. \tag{3}$$

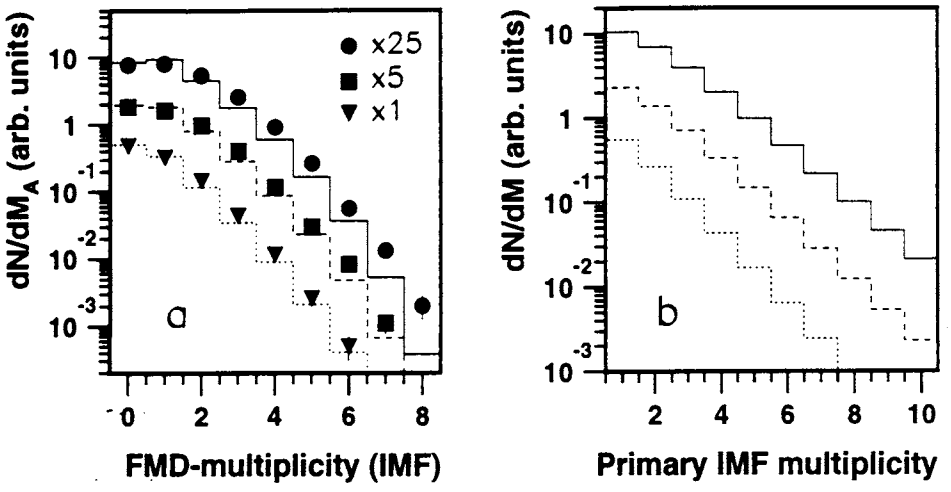

Fig.1. Left: measured IMF-multiplicity distributions associated with a trigger fragment of charge $6 \le Z \le 20$ for p + Au collisions at 8.1 GeV (circles, solid line), 3.6 GeV (squares, dashed line), 2.16 GeV (triangles, dotted line). They are fitted with Fermi-like primary distributions (right picture), folded with the experimental filter

The right side of this equation can be also found from the coincidence rate n_{12} for IMF's in the triggering telescopes:

$$\frac{n_{12}}{n_1 p_2} = \frac{\langle M^2 \rangle}{\langle M \rangle} - 1. \tag{4}$$

Here n_1 is counting rate in telescope 1, p_2 is the detecting probability for the coincident fragment in telescope 2. Using eqs.(3) and (4) one can find the efficiency of the fragment multiplicity detector ε. This is the way to control the calculation of ε:

$$\varepsilon = \langle M_A \rangle \frac{n_1 p_2}{n_{12}}. \tag{5}$$

We used the coincidence data for the telescopes located at θ equal to 68°, 87°, and 112°. For that geometry the probability p_2 is largely determined by the solid angle of telescope 2. The correction for the IMF-IMF angular correlation is around 6%. The FMD efficiency found with (5) differs only by 7% from the calculated one, and that is within the counting rate statistics of coincidences.

How to get the primary multiplicity distribution $W(M)$ from the measured one $W(M_A)$? The first way is fitting the parametrized $W(M)$, folded by the experimental filter according to (1), to the experimental distribution. It was done assuming $W(M)$ to be shaped like a Fermi function. This choice was motivated by calculations using the statistical model of multifragmentation (see below). The results are presented in Fig.1b. The mean values of the primary IMF multiplicities (for the events with at least one IMF) are equal to 1.7 ± 0.2,

1.9 ± 0.2, and 2.1 ± 0.2 for the beam energies 2.16, 3.6, and 8.1 respectively. These values are slightly lower than obtained in paper [14] because a higher FMD efficiency was used*.

Another way (a bit more complicated) is direct reconstruction of $W(M)$ using the reverse matrix $Q^{-1}(M, M_A)$:

$$W(M) = \sum_{M_A=0}^{M-1} Q^{-1}(M, M_A)\, W(M_A). \qquad (6)$$

The matrix Q^{-1} is obtained by solving the equation $Q \cdot Q^{-1} = 1$. Directly reconstructed $W(M)$ are close in shape to those shown in Fig.1b. They are presented in Fig.2 together with the ones calculated by the statistical multifragmentation model.

Comparison with Model Calculations

The reaction mechanism for the relativistic projectiles is divided into two steps. The first one consists of a fast energy deposition stage, during which very energetic light particles are emitted and the nuclear remnant (spectator) is excited. The second one is the decay of the target spectator. The fast stage is usually described by the intranuclear cascade model (INC). We use a version of the INC from Ref.18 to get the distributions of the nuclear remnants in charge, mass and excitation energy. The second stage is described by the statistical multifragmentation model (SMM) [19]. The statistical behaviour of the target spectator is evident from the fact that the angular distributions of IMF's and their energy spectra at different angles are well described in the framework of the statistical decay of a thermalized moving source [20]. Within the SMM the probabilities of different decay channels are proportional to their statistical weights. The break-up volume determining Coulomb energy of the system is taken to be $V_b = (1 + k)A/\rho_0$, where A is the mass number of the decaying nucleus, ρ_0 is the normal nuclear density, k is a model parameter. So, thermal expansion of the system before the break-up is assumed. The primary fragments are hot, and their deexcitation is taken into account to get final IMF distributions. In further calculations we use $k = 2$ based on our analysis of the correlation data [12]. This value corresponds to the break-up density $\rho_b \approx 1/3\rho_0$. The upper dashed line in Fig.3 is obtained by means of this combined model. The calculated mean multiplicity for the highest energy is almost two times larger than the experimental one indicating a significant overestimation of the excitation energy of the residual nucleus. For the lowest beam energy the calculated mean multiplicity is still larger than the experimental one though not so much.

The shortcoming of the INC algorithm is that the exciton approach doesn't provide a reliable calculation of excitation energy in case when many nucleons are involved in the cascade stage. The use of the preequilibrium exciton model (PE) [21] together with the INC results in significant decreasing excitation energy of the target spectator and reducing mean IMF multiplicities (lower dotted line in Fig.3). The calculated value of $\langle M \rangle$ at the beam

*In the light of these results the IMF multiplicities in helium-induced reaction [5] were remeasured: $\langle M \rangle = 2.2 \pm 0.2$ for 14.6 GeV.

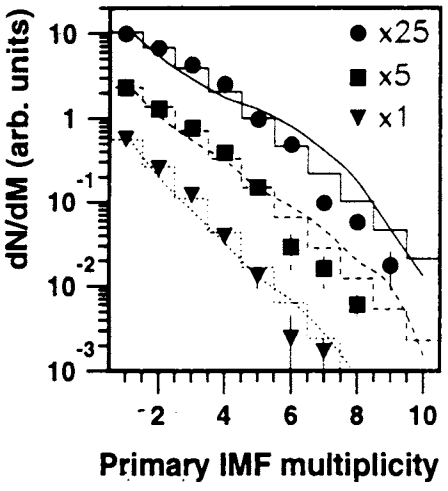

Fig.2. Primary IMF distributions. Symbols are for directly reconstructed distributions: circles, squares and triangles are for the beam energies 8.1, 3.6, 2.16 GeV respectively. Histograms are from Fig.1b, the smooth lines are calculated with the statistical multifragmentation model (see the text)

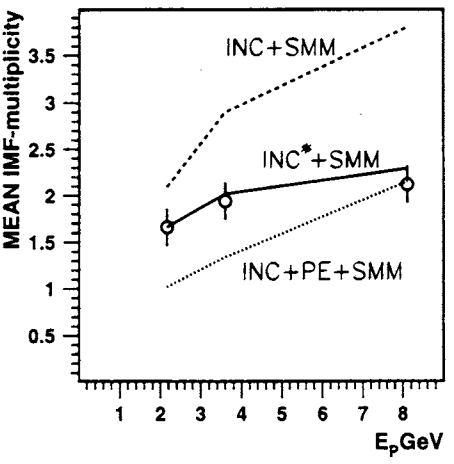

Fig.3. Mean IMF multiplicities as a function of the beam energy. Open points are experimental data. Dashed and dotted lines are drawn through the values calculated with INC + SMM and with INC + PE + SMM at the beam energies used. The solid line is obtained with the use of modified INC* followed by SMM

energy of 8.1 GeV coincides with the experimental one, but, as will be shown below, the model-predicted fragment kinetic energies are significantly lower than the measured ones. It means that the model underestimates the Z value of the target residue, as the fragment kinetic energies are determined in the main by the Coulomb field of the source [12]. With decreasing beam energy, the calculated mean IMF multiplicities fall rather fast approaching 1 at $E_p = 2.16$ GeV. The reason for that is the model underestimation of the spectator excitation energy. So, the use of the INC or INC + PE does not solve the problem of describing the properties of a target spectator for a wide range of projectile energies, and one should look for an alternative approach. The authors of [22] came to a similar conclusion and used some phenomenological distributions of the mass numbers and the excitation energies of a source to describe multifragmentation of spectators in relativistic heavy-ion reactions.

The solid line in Fig.3 was calculated using the empirical modified intranuclear cascade model (INC*) followed by SMM. In this modification the masses and charges of the residual are kept unchanged, as given by INC, but the excitation energies are α times reduced. The parameter α was taken to be equal to the ratio of the experimental mean IMF multiplicity to the calculated one in INC + SMM:

$$\alpha = \frac{\langle M_{\text{exp}} \rangle}{\langle M_{\text{INC + SMM}} \rangle} . \qquad (7)$$

Table. The calculated properties of the nuclear remnants in p + Au collisions

E_p, GeV	Exper. $\langle M_{IMF} \rangle$	Calculations							Model
		$\langle M_{IMF} \rangle$	Z_R	A_R	Z_{MF}	A_{MF}	E_R^*	E_{MF}^*, MeV	
8.1	2.1 ± 0.2	3.80	74	180	70	168	524	911	INC + SMM
		2.15	67	163	50	121	204	526	INC + PE + SMM
		2.29	74	180	69	164	289	591	INC* + SMM
3.6	1.9 ± 0.2	2.90	76	185	73	176	407	757	INC + SMM
		1.34	70	171	55	134	148	385	INC + PE + SMM
		2.02	76	185	73	174	285	582	INC* + SMM
2.16	1.7 ± 0.2	2.09	77	188	75	181	328	642	INC + SMM
		1.02	72	176	62	145	119	266	INC + PE + SMM
		1.66	77	188	75	180	262	543	INC* + SMM

Z_R, A_R, E_R^* are the charge, mass number and excitation energy averaged over all the target spectators.
Z_{MF}, A_{MF}, E_{MF}^* are the same, but averaged over the residues decaying with IMF emission.

This is motivated by the model correlation between $\langle M \rangle$ and the spectator excitation energy. We are aware that such a modification must be accompanied by corresponding changing of parameters of the cascade outgoing particles. However in the present paper we are concentrated only on reproduction of multifragmentation phenomena. So, the solid curve in Fig.3 is obtained with the parameter α equal to 0.8, 0.7, and 0.55 for the beam energies 2.16, 3.6, and 8.1 GeV respectively. It goes very close to the data.

The table summarizes the results of the calculations. Note that according to the INC* + SMM model, the mean excitation energy of the residues E_R^* is changed only slightly (from 285 to 289 MeV) when the beam energy varies from 3.6 to 8.1 GeV. This saturation effect was noted already in papers [7,8] for ^{3}He interactions (up to 4.8 GeV) with silver. The IMF emission takes place on the tail of the excitation energy distribution, therefore the mean excitation of the fragmenting nuclei is approximately twice as large.

The model-calculated IMF multiplicity distributions (for the case of INC* + SMM) are shown in Fig.2 together with the reconstructed experimental ones.

Energy Spectra and Charge Distributions of IMF

Figure 4 presents the comparison of the mean kinetic energies of fragments (measured at the beam energies of 2.16 and 8.1 GeV) with the calculated ones. The data are obtained with the telescope located at $\theta = 87°$ and corrected for the detection threshold (E/A = 1.2 MeV). The measured mean energies for the lower beam energy are slightly higher than

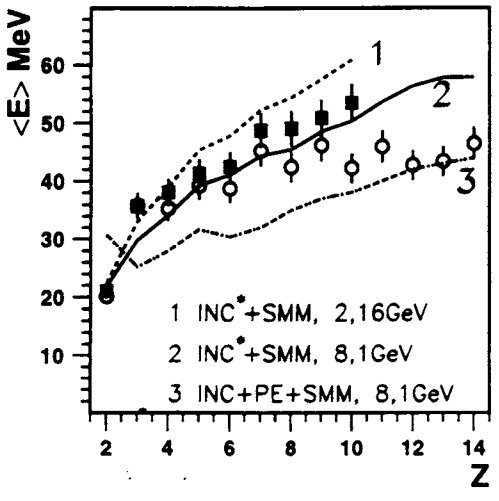

Fig.4. Mean kinetic energies of fragments in p + Au collisions at 2.16 GeV (solid points, line 1) and 8.1 GeV (open points, lines 2,3). The lines are calculated with modified INC* + SMM (1,2) and INC + PE + SMM (3)

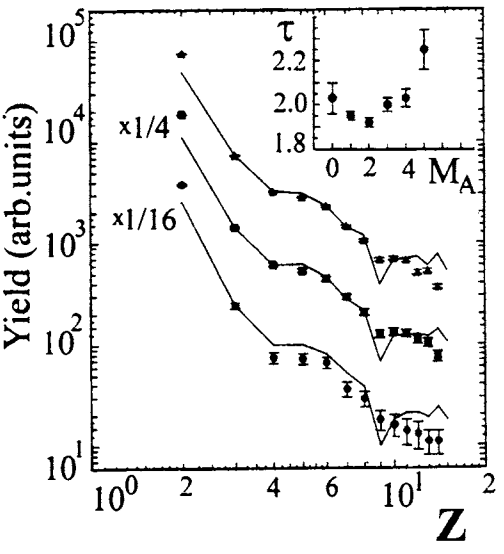

Fig.5. Fragment charge distributions measured at $\theta = 87°$ for the beam energies 8.1 GeV (top), 3.6 GeV (middle) and 2.16 GeV (bottom). The lines are calculated by INC* + SMM (normalized at $Z = 3$). The insert gives the τ-parameter deduced from the IMF-charge spectra for the beam energy 8.1 GeV

those for $E_p = 8.1$ GeV. This is caused, in the main, by the larger charge of the decaying nucleus for the lower beam energy.

Let us first consider the region $Z_{IMF} \leq 9$. The calculations using the INC + PE + SMM model for $E_p = 8.1$ GeV give definitely lower mean energies than the experimental ones indicating the model underestimation of the target spectator Z and A. The calculated mean energies are close to the data when modified INC* followed by SMM is used. For $E_p = 2.16$ GeV, Fig.4 presents the results obtained with the modified intranuclear cascade model. The calculated values are slightly above the experimental ones.

Let us consider the data for heavier fragments shown for $E_p = 8.1$ GeV. For $Z > 9$ IMF-energies practically do not change in contrast to the model prediction. It could be explained by dominating of channels with small number of IMF's. For these channels the break-up volume may not be constant and may increase with the IMF's size; it needs an additional analysis. Another possible explanation of this observation is the failure of the SMM assumption that the fragments have equal probabilities to be formed at any available place inside the break-up volume. In fact, the interior of the expanded nucleus is favoured over the diffuse edge for the appearance of larger IMF's as the fragments are formed via the density fluctuations. This results in lower Coulomb energies for them with respect to

the model prediction. This observation presents additional evidence for the volume emission of the fragments. A similar conclusion was made in [23].

Figure 5 shows the charge distributions of IMF's. The calculations in the INC* + SMM model resemble the general behaviour of the data. The empirical power law $Y(Z) \sim Z^{-\tau}$ describes the data also well. In the insert of Fig.5 the dependence of the τ-parameter on the associated IMF-multiplicity M_A is shown: with increasing multiplicity, the τ-parameter goes down and further goes up. In the earlier papers on the multifragmentation [23,24] the power law for the fragment charge yield was interpreted as an indication of the proximity to the ciritical point for the liquid-gas phase transition in nuclear matter. But in fact the fragmenting system is not so close to the critical point [25] and one should look for a less exotic explanation of the power law behaviour of $Y(Z)$. Probably a convenient interpretation can be found in a more correct consideration of the secondary decay of excited fragments. As was already mentioned, the IMF multiplicity is correlated with the excitation energy of the system. For the low multiplicities the system is close to the evaporation regime. In this case increasing excitation energy results in enhancement of the yield of heavier fragments (τ falls down). As the excitation continues increasing, the secondary decay of the fragments becomes more significant, enhancing the yield of lighter fragments (τ goes up).

It was mentioned in the introduction that the IMF + IMF angular correlation gives important information on the emission time. In this work we obtained a correlation function $R(\theta_{12})$ from the coincidences between the trigger telescopes and the PM's of the fragment multiplicity detector at the beam energy of 8.1 GeV. The correlation function shows a minimum at $\theta_{12} \approx 0$ caused by the Coulomb repulsion between fragments. The magnitude of the small angle suppression is practically the same as for collisions ^{4}He (14.6 GeV) + Au [12,13]. This means that the IMF emission time for proton-induced multifragmentation does not exceed 100 fm/c as in collisions He + Au. Detailed analysis of the angular correlations will be presented in a separate publication.

Conclusion

Multiple emission of intermediate mass fragments has been studied for the collisions p + Au at the beam energies 2.16, 3.6, and 8.1 GeV with the modified FASA set-up. The mean IMF multiplicities are equal to 1.7 ± 0.2, 1.9 ± 0.2, and 2.1 ± 0.2 respectively. The intranuclear cascade calculations with or without preequilibrium emission do not solve the problem of describing the properties of a target spectator for the projectile energies used. The epxerimental data on the IMF multiplicity and charge distributions as well as fragment kinetic energies are described with the empirically modified intranuclear cascade calculations followed by the statistical multifragmentation model. The present data support a scenario of true thermal multifragmentation of a hot and expanded nuclear system.

The authors are thankful to Prof. A.Hrynkiewicz, A.M.Baldin, S.T.Belyaev and E.Kankeleit for support. The research was supported in part by Grant No.RFK300 from the International Science Foundation and Russian Government, Grant No.96-02-18952 from Russian Foundations for Basic Research, by Grant No.94-2249 from INTAS, by Grant

No.P30B 09509 from Polish State Committee for Scientific Research, by Contract No.06DA453 with Bundesministerium für Forschung und Technologie and by the US National Science Foundation.

References

1. Lynch W.G. — Ann. Rev. Nucl. Part. Sci., 1987, v.37, p.493.
2. Moretto L.G., Wozniak G.J. — Ann. Rev. Nucl. Part. Sci., 1993, v.43, p.379.
3. Bondorf J.P. et al. — Phys. Reports, 1995, v.257(3), p.133.
4. Avdeichikov V.V. et al. — Yad. Fiz., 1988, v.48, p.1796.
5. Lips V. et al. — Phys. Rev. Lett., 1994, v.72(11), p.1604.
6. Pienkovski L. et al. — Phys. Lett., 1994, v.B336, p.147.
7. Morley K.B. et al. — Phys. Rev., 1996, v.C54(2), p.737.
8. Foxford E.R. et al. — Phys. Rev., 1996, v.C54(2), p.749.
9. Viola V.E., Kwiatkowski K. — Progress Report INC-40007-112, Indiana University, Bloomington, 1996.
10. Tanaka K.H. et al. — Nucl. Phys., 1995, v.A583, p.581.
11. Schapiro O., Gross D.H.E. — Nucl. Phys., 1994, v.A573, p.143.
12. Shmakov S.Y. et al. — Yad. Fiz., 1995, v.58(10), p.1735; (Phys. of Atomic Nucl., 1995, v.58(10), p.1635).
13. Lips V. et al. — Phys. Lett., 1994, v.B338, p.141.
14. Karnaukhov V.A. et al. — JINR Preprint E1-96-50, Dubna, 1996.
15. Avdeyev S.P. et al. — Pribory i Tekhnika Eksper., 1996, v.39(2), p.7; (Instr. Exp. Techn., 1996, v.39(2), p.153).
16. Avdeyev S.P. et al. — Nucl. Instr. Meth., 1993, v.A332, p.149.
17. Stracener D.W. et al. — Nucl. Instr. Meth., 1990, v.A294, p.485.
18. Toneev V.D., Gudima K.K. — Nucl. Phys., 1983, v.A400, p.173c.
19. Botvina A.S., Iljinov A.S., Mishustin I.N. — Nucl. Phys., 1990, v.A507, p.649.
20. Karnaukhov V.A. et al. — In: Proc. of Int. Conf. «Low Energy Nucl. Dynamics» St. Petersburg, ed. Yu. Oganessian, World Scientific, Singapore, 1995, p.423.
21. Blann M. — Ann. Rev. Nucl. Sci., 1975, v.25, p.123.
22. Botvina A.S. et al. — Nucl. Phys., 1995, v.A584, p.737.
23. Hirsch A.S. et al. — Phys. Rev., 1984, v.C29, p.508.
24. Siemens P.J. — Nature, 1983, v.305, p.410.
25. Karnaukhov V.A. — JINR Preprint E7-96-182, Dubna, 1996; Yad. Fiz., 1997, v.60(10).

Received on February 27, 1997.